Chemical bath deposition of CZTS layers; study of pH, time deposition and annealing temperature effects

D. Haouanoh [a], M. Toubane [a,*], R. Talaighil [a], F. Bensouici [b]
[a] UR-MPE Unit, University M`Hamedbougaraboumerdes, 35000 Boumerdes, Algeria
[b] Science of matter department, ABBAS Laghrour University, Khenchela 40004, Algeria

CZTS thin layers were successfully deposited onto both glass and indium-tin oxide substrates using the chemical bath deposition method. The effects of solution pH, deposition time, and annealing temperature on the structural, morphological, and optical properties were investigated. Thermal analysis (DSC/TGA) shows that the CZTS kesterite structure crystallized at 237.2°C. Structural analysis by X- ray Diffraction, Rietveld refinement and Raman spectroscopy, revealed that the kesterite phases formation with the presence of SnO_2cassiterite and ZnO wurtzite structures in the films annealed at a higher temperature with nanocrystalline size. SEM images showed smooth and homogeneous surfaces, with the presence of cracks and voids. All films present high absorption in the visible ranges. The solution's pH and the annealing temperature significantly impact the calculated band gap. In contrast, the deposition time does not notably affect the film quality.

1. Introduction

In recent years, research on photovoltaic cells is based on non-toxic and with low cost thin-layer solar cells; especially Cu_2ZnSnS_4 (CZTS) based cells. The combination of three metalslike copper, zinc and tin with sulfur, gives us a p-type CZTS semiconductor with 1.50 eV gap energy and an absorption coefficient of 10^4 cm^{-1}in visible spectrum range[1], This is why this material is consecrated as the best absorber for solar radiation.

Several physical and chemical techniques are required by different researchers to develop CZTS thin films. Among the physical methods one can cite: vacuum thermal evaporation [2, 3], co evaporation[4], RF magnetron sputtering [5, 6]. Hybrid sputtering [7]. The use of these methods makes it possible to obtain interesting conversion efficiency. For example; the thermal evaporation in a vacuum system deposit gave a conversion efficiency of 8.4%[8].RF magnetron sputtering technique provided 6.7% efficiency [9]. A conversion efficiency of 11.6% is achieved by the use of the co-evaporation technique [10]. The problem that arises in the use of the physical methods that these techniques require more sophisticated and expensive equipment; on the other hand, the chemical techniques are simpler and less expensive methods for depositing CZTS layers. These methods include, spray pyrolysis [11, 12], spin coating [13, 14], SILAR method sulfurizing [15] and chemical bath deposition CBD [16, 17]. The latter is a simple process, inexpensive and safe [18], no sophisticated instrument is required [19], used to obtain homogeneous and adherent thin films reproducible on large surfaces. It is considered as an excellent technique for thenano-crystals deposition[19, 20].   Deposition CBD has the potential to be used for the production of CZTS solar cells and conversion efficiency about 4.5% and 1.34% were reported[21, 22]. In this technique, several parameters must be checked to attain good quality CZTS thin films for example; pH of solution, deposition temperature, time deposition, annealing temperature, annealing time...etc.

In this study, Cu₂ZnSnS₄ solution is prepared by new process to deposit thin layer czts by CBD technique into glass and ITO. The effect of the pH solutions, the time deposition, and the annealing temperature were investigated to determine the structural, the morphological and the optical properties CZTS   films for cell solar application.

2. Experimental part

2.1. Materials and characterization

Copper chloride dehydrate CuCl₂·2H₂O zinc chloride ZnCl₂, tin chloride dehydrate SnCl₂·2H₂O (thiourea CS(NH₂)₂ were used as copper, zinc, tin source and sulfur sources, respectively. Methanol alcohol (70% reagent) was used as the solvent and monoethanolamine served as the complexion agent.

The differential scanning calorimetric and thermogravimetric (DSC/TGA) STA 409 PC is used to analyses the CZTSxerogel. X-ray diffractometer type Philips X'Pert with theta-2 theta geometry equipped with Cu-kα radiation source is employed to determine the CZTS thin films structural properties. The surfaces morphology is characterised by the Electron Microscope Versa 3D. Meanwhile, UV-Visible Perkin Elmer Lambda EZ210 measured the optical transmission and absorption spectra.

2.2. Thin films' deposition

Cu₂ZnSnS₄ layers were grown by chemical bath deposition (CBD) onto glass and indium-tin oxide (ITO) substrates that were cleaned ultrasonically. The chemical bath consisted of an aqueous solution containing copper(II) chloride dehydrate 0.032 M, zinc chloride 0.016 M, tin(II) chloride dehydrate 0.016 M, and thiourea 0.128 M. These components were dissolved in 50 mL of methanol. To adjust the pH of the solution, monoethanolamine was added. (Table 1). Fig.1. represents the steps of the chemical bath preparation. The complex reactions are summarized as follows[23].

$$2CuCl_2 . \ 2H_2O + 4CH_3OH = 2Cu^{2+} + 4CH_3O^- + 4HCl + 4H_2O$$
$$ZnCl_2 \ + 2CH_3OH = Zn^{2+} + 2CH_3O^- + 2HCl + 2H_2O$$
$$SnCl_2 \ + 2CH_3OH = Sn^{2+} + 2CH_3O^- + 2HCl + 2H_2O$$
$$CS(NH_2)_2 \ + 4CH_3OH = 4S^{2-} + 12H^+ + N \equiv C\text{-}NH_2 + 2CH_3O^-$$
$$2Cu^{2+} + Zn^{2+} + \ Sn^{2+} + 4S^{2-} \ = Cu_2ZnSnS_4$$
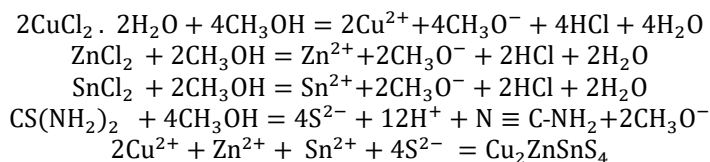
Table 1. Different pH with various MEA volumes.

pH	7.1	7.8	8.5
MEA (0.82M)	6ml	7ml	8ml
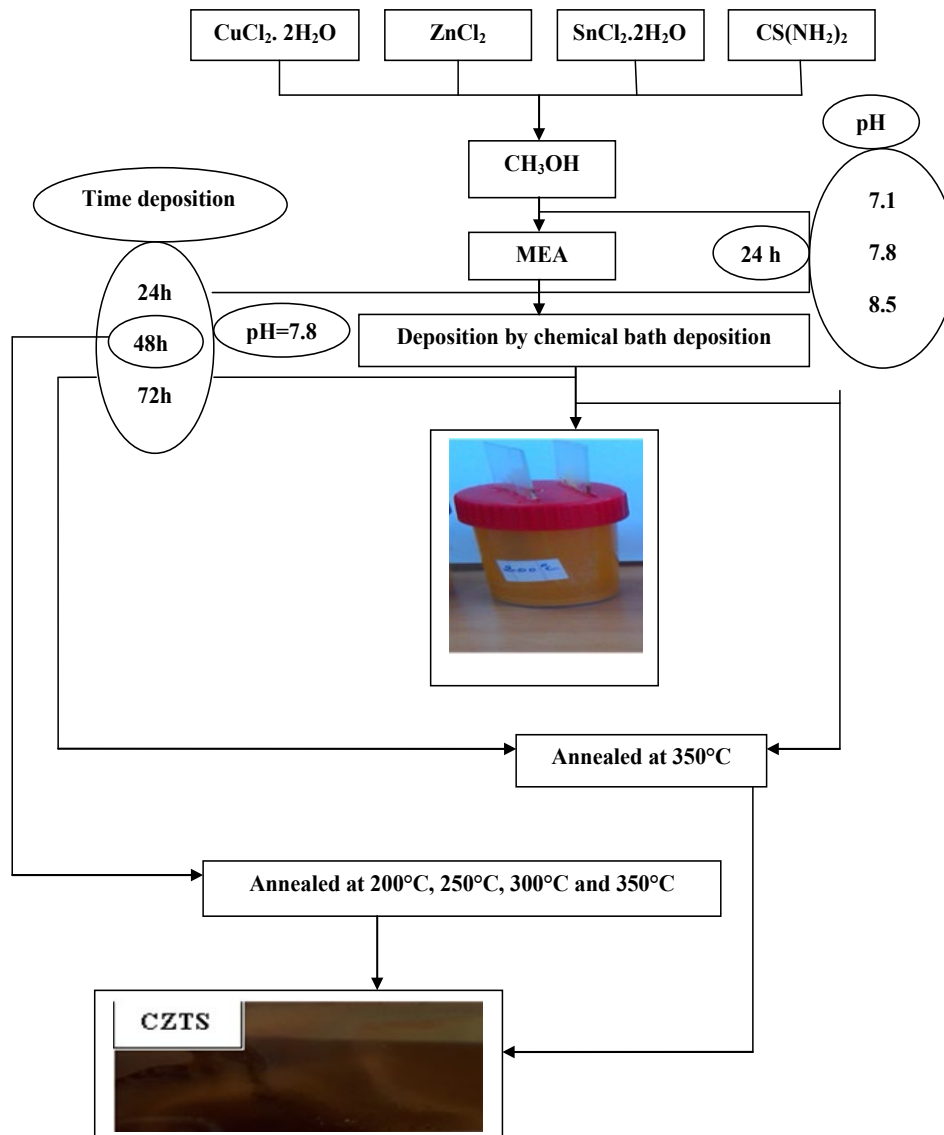
Fig. 1. Steps of chemical bath preparation.

3. Results and discussion

3.1. Thermal analysis

Fig.2. shows DSC and GTA analysis for obtained xerogel once the aqueous solution has been dried at 100 $^\circ$C. It can be seen that there are two endothermic peaks at 169.2ºC and 223.9ºC, accompanied by a 3.35% and 45.91% weight loss, which correspond to the evaporation of the mono-ethanolamine and the decomposition of Cyanamid (CSNH$_2$) in C and NH$_2$. One can observealso the presence of three exothermic peaks at 237.1ºC, 260.0ºC and 279.3ºC can be attributed to the CZTS, the SnO$_2$ and the ZnO crystallization respectively. The crystallization of the metal oxide can be explained by the sulfur evaporation and the combination of metal and atmospheric oxygen.
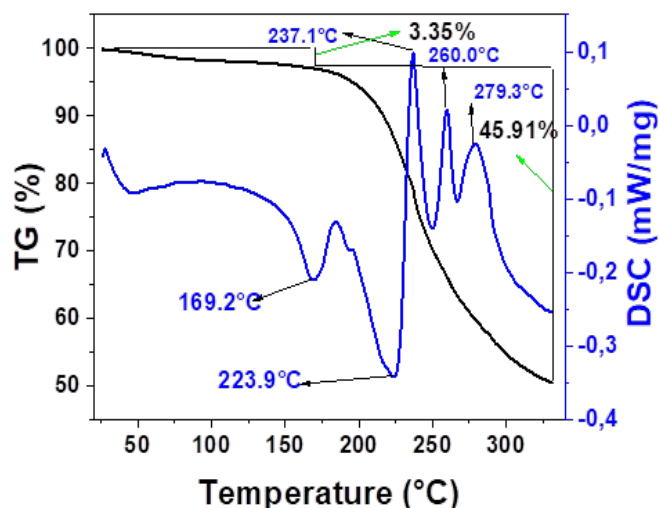
Fig. 2. Differential scanning calorimetric and thermo-gravimetric (TGA/DSC) analysis.

3.2. Structural properties

3.2.1. pH effect

Fig.3.a) shows theX-ray diffraction spectrafor CZTS layers deposited at different pH values (7.1, 7.8 and 8.5). It can be seen that the presence of three peaks corresponding to the planes from (112), (220) and (312) indicating that the kesterite CZTS structure formation with (112) as the preferential orientation (JCPDS card number 96-900-4751). This result is in accordance with the preceding researches [24, 25]. The intensity of the peaks decreases as pH increases values form 7.1 to 7.8. This enhancement can be explained by the increasing of ($\overline{N}H_2$, Lewis base)in the solution results in elevated of pH values, the presence of more $\overline{N}H_2$ than H^+ ions will accelerate the hydrolysis of thiourea ($CS(NH_2)_2$) which than liberates sulfur (S^-) ions to form CZTS compound. Beyond pH value 7.8, the intensity of the peaks decreases with increasing pH values (7.8 to 8.5), this result is due to the $\overline{N}H_2$ excess in the solution that results in higher pH value.The acceleration of thiourea hydrolysis accelerates the precipitation of CZTS nano-particles and the decrease in the deposit rates. It can also be observed the presence of the casseterite SnO_2 structure (JCPDS card number 96-900-9083) secondary phase.The existence of this phase is due toevaporation of the sulfur and its combination with tin (Sn) and the atmospheric oxygen.

3.2.2. Time deposition effect

The X-ray diffraction pattern of CZTS layers deposited at various time deposition (24h to 72h) are shown in fig.3.b), one can see that the existence of diffraction peaks situated at 28.5°, 47.5° and 56.2° corresponding to (112), (220) and (312) plains. The formation of kesterite phase was observed in these peaks, with (112) being the preferred orientation according to the JCPDS card Nº. 96-900-4751, the appearance of SnO_2 secondary phase in all films and ZnO secondary phase in the film deposited at 72h time deposition are observed, the presence of these phases is due to the evaporation of sulphur and combination of metal and atmospheric oxygen. The intensity of peaks increase with increasing time deposition, this increase can be clarified by the increasing of thickness.

3.2.3. Effect of annealing temperature

The spectra presented in Fig. 3.c are similar to those of CZTS thin layers annealed at various temperatures. It can be observed that the films were heated at 200°C and 250°C. present only the peaks reflection (112), (220) and (312) plans corresponding to kesterite CZTS structure (JCPDS card number 96-900-4751). Beyond 250°C, we can be noticed that the presence of other peaks corresponding to the (110), (101) and (211) plains indicating cassiterite SnO_2 structure formation. At 350°C another peak is appeared at 31.2° correspond to (100) plain indicate the formation of ZnO structure.
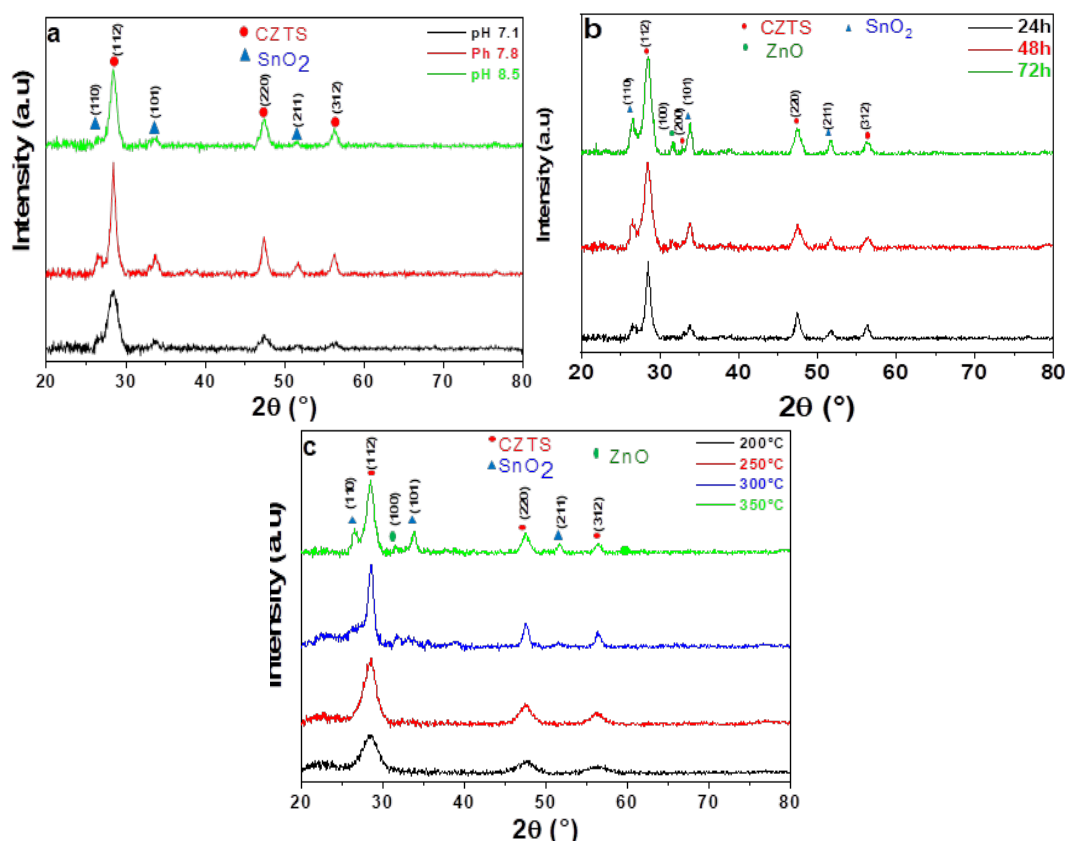
Fig. 3. XRD Spectrum of CZTS layers prepared at various parameters,
a) pH solutions, time deposition and c) annealing temperature.

3.3. Rietveld refinements

The Rietveld refinements were approved using a (CZTS)kesterite tetragonal structure that incorporates the space group I42/m (121) and SnO_2cassiterite tetragonal structure with space groupP42/mnm (136), the results are displayed in the table (2, 3 and 4). Both micro-structural parameters (crystallite size and microstrain) and lattice parameters (a and c) were refined. Fit parameters Rwp (%) are weighted in the profile, R-factor; R_p (%) profile R-factor; R_e (%) expected R factor; $S = R_{wp}/R_e$ and $\chi^2 = S^2$ goodness of fit) indicate a good fit. We can be observed that the value of R_{wp} and R_p are slightly large, This is because of the low diffraction peak to background ratio value, due to the nanocrystalline nature presence[26, 27]. Though, a small goodness value of fit (χ^2) has been seen which reflectsan optimized refinement. The lattices parameters values that are shown in Table (2,3 and4) are closer to the values reported in the literature. The crystallites size affected by the three parameters to study: (i) increases with the pH values increase from(7.1 to 7.8) (see table 2) can be due to the crystallization improvement the quantity of crystallographic flaws, such as dislocations, vacancies, and interstitials in CZTS layers reduction[28]. Beyond pH 7.8 the crystallites size decreases with increasing pH values.

Table 2. Rietveld parameters and band gap energy of CZTS layers prepared at different pH solutions.

pH	Crystallite size (nm)	Microstrain (%)	Lattice parameters (Å)	R_{wp}(%)	R_p (%)	R_e(%)	S	X^2	E(eV)
7.1	4.54	3.451	5.425(9)/10.605(2)	16.41	14.78	14.27	1.15	1.322	1.74
7.8	11.81	1.320	5.422(4)/10.745(1)	15.37	13.16	14.12	1.08	1.185	1.58
8.5	6.20	2.522	5.427(4)/10.771(6)	13.01	10.84	12.28	1.06	1.123	2.23

ii) Concerning time deposition (see table 3), the crystallites size decrease (from 11.81 nm to 6.20 nm) with time deposition from (24h to 48h) however they increase with increasing time deposition Beyond 48h.

Table 3. Rietveld parameters and band gap energy of CZTS layers prepared at various time deposition.

Time (h)	Crystallite size (nm)	Microstrain (%)	Lattice parameters (Å)	R_{wp}(%)	R_p (%)	R_e(%)	S	X^2	E(eV)
24	11.810	1.320	5.422(4)/10.745(1)	15.37	13.16	14.12	1.08	1.185	1.58
48	5.864	2.679	5.373(0)/10.864(0)	16.19	15.08	10.10	1.50	2.666	1.61
72	6,150	2.548	5.401(4)/10.771(4)	10.16	9.30	9.71	1.04	1.094	1.60

For annealing temperature low then 300°C, crystallites size increase with this raise can be explained by crystallization improvement and the crystallographic defects density dipping. Further than 300°C the crystallites size decreases (from 9.918 nm to5.864 nm) with temperature rising (from 300°C to 350°C) (refer to Table 4).

Table 4. Rietveld parameters and band gap energy of CZTS layers prepared at various annealing temperature.

Temperature (°C)	Crystallite size (nm)	Microstrain (%)	Lattice parameters (Å)	R_{wp}(%)	R_p (%)	R_e(%)	S	X^2	E(eV)
200 °C	4.004	3.940	5.421(9)/10.628(4)	12.20	10.58	9.97	1.22	1.496	2.29
250 °C	4.641	3.382	5.423(1)/10.692(4)	10.17	9.10	9.89	1.02	1.056	1.54
300 °C	9.918	1.576	5.394(2)/10.842(4)	13.64	12.16	9.97	1.37	1.871	1.63
350 °C	5.864	2.679	5.373(0)/10.864(0)	16.19	15.08	10.10	1.50	2.666	1.61

3.4. Raman spectroscopy

In order to validate the X-ray diffraction results, Raman spectroscopy was used to characterize the CZTS thin films annealed at different temperatures. Raman scattering spectra of CZTS layers which are excited by laser radiation with a wavelength of 325 nm are shown in Fig.4. All spectra confirm the presence of the kesterite CZTS phase for all films, by the presence of two main photos located at 288 Cm^{-1} and 338 Cm^{-1} attributed to the A1 vibration mode. We also notice the appearance of two secondary peaks at 99 Cm^{-1} and 315 Cm^{-1}[29, 30] corresponding to the vibration modes B and E respectively. Another peak at 561 Cm^{-1}which does not match the CZTS structure, the presence of this peak may be due to the nanocrystals constituting the CZTS thin layers.
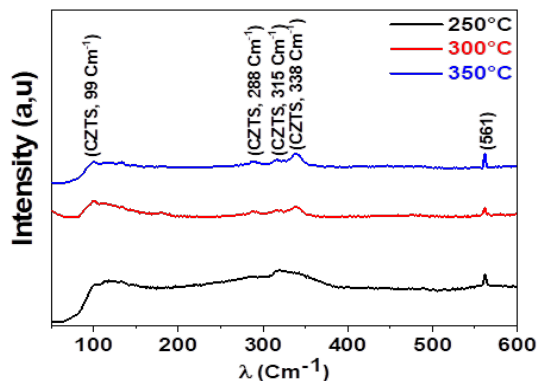
Fig. 4. Raman spectra of CZTS layers heated at various temperature (250 ° C, 300 ° C and 350 ° C).

3.5. Surface morphology

Figure.5. Show the SEM images CZTS thin layers using scanning electronic microscopy Versa 3D, (Figure 5, 24h (a) shown that a distribution of small grain of CZTS particles. With increasing of time deposition we can be notice that an agglomeration of CZTS grains. The image (48h (c) shows a cracking of CZTS layers prepared at 48h time deposition, we can be seen the phenomenon of sedimentation, this result can be explained by the principle of deposit method (CBD).In order, a backscattered (BSE) detector was used on scanning electron microscope (Versa 3 D) for detect the composition contrast (Figure 5, (24h (b) and 48h (b)), clearly indication of the presence of two phases (CZTS and SnO2) for the CZTS thin film surface that was created in 24 h, and three phases (CZTS (white grains) , SnO_2 (grey grains) and ZnO black grains) for the surfaces of CZTS layer prepared at 48h.
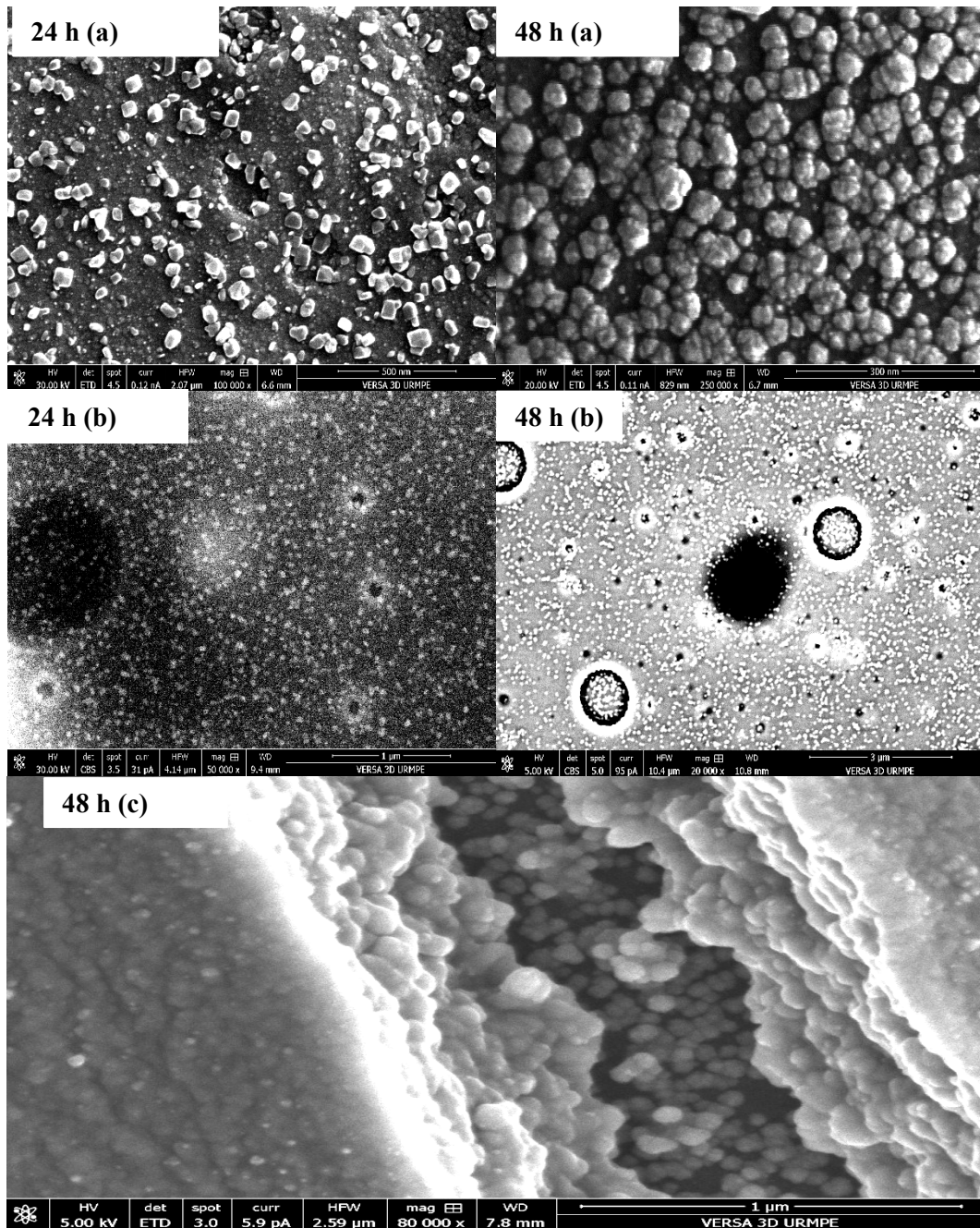
Fig. 5. SEM pictures of CZTS thin films made at various time deposition.

3.6. Optical properties

The CZTS layers transmission and absorptions spectra are shown in fig.6. It seems that the parameters taken into consideration have a significant impact on both transmission and absorption, such as pH solution, time deposition and annealing temperature. The CZTS layers absorption band gap edge is estimated as of the derivate of the transmittance spectra (dt/dλ), as represented in figure. 8, and determined using the equation that follows [31].

$$Eg = \frac{hc}{\lambda \max(\text{Å})} \tag{1}$$

where Eg is the Band gap energy, c is velocity of light, h is the planck's constant and λ is the wavelength at which the first derivative is maximum.

3.6.1. pH effect

From fig.6.a,d) one can see that in the transmittance decreases with increasing pH values until60%, in contrary of absorption. These results can be explained by the thickness enhancement and by increasing the deposit rate. Similar behaviors are found by Ferhat Aslanet al. [32].Beyond the 7.8 value, the transmittance augments and the absorption is reduced. It can be explained the diminution of deposit rate. The values of band gap as function pH value are illustrated in table 2. The band gap decreases (1.74 to 1.58 eV) as the pH rises from 7.1 to 7.8. This can be explained by the deposit rate enhancement. For pH values are greater than 7.8, the energy gap increasing.

3.6.2. Time deposition effect

It can be observed that from (fig.6.b,e) the transmittance decreases with increasing time deposition, contrary of the absorption which is raised with raising time deposition. These results can be explained by raising the thickness. There is no great influence of time deposition on the band gap energy (see table 3).

3.6.3. Annealing temperature effect

One can see that fig.6.c.f) the transmittance decreases 35% and consequently the absorption increases as the annealing temperature increases (200ºC to 300ºC) within the range of visibility, this result is due to the crystallization at higher temperature improvement . Beyond 300ºC,there is an enhancement of transmission 46%due to the metals oxides SnO_2 and ZnO appearance with high transmittance and low absorbance in visible range [33, 34]. Table 4 displays the band gap energy values as a function of the annealing temperature; one can notice that the band gap decreases from 2.29 to 1.54 eV with annealing temperature increases (200ºC to 250ºC). This is due to kesterite structure crystallization improvement. Above 250ºC, the band gap enhances with annealing temperature improvement. This result can be clarified by higher SnO_2 and ZnO band gap energy [35, 36].
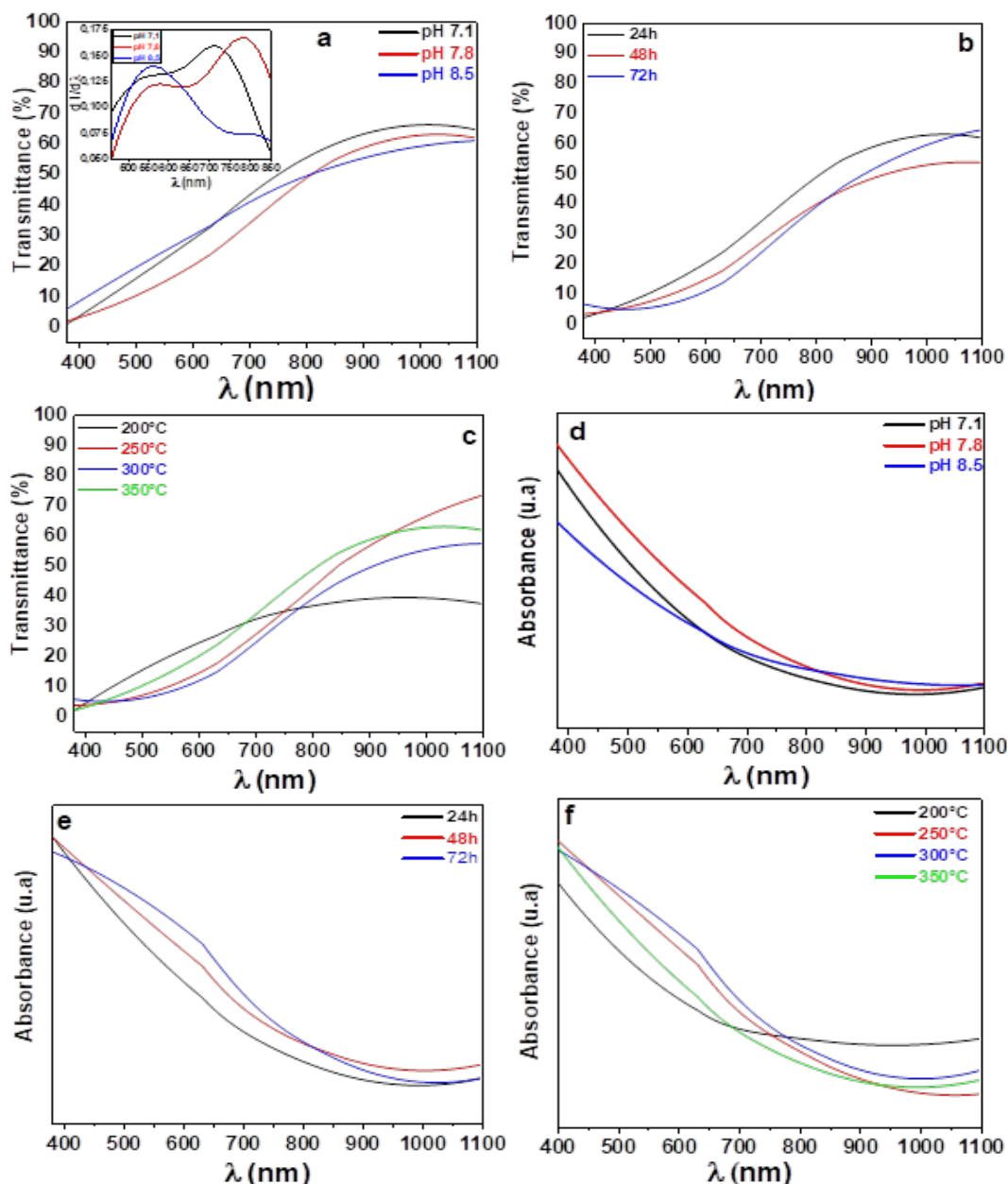
Fig. 6. CZTS thin film transmittance and absorbance spectra produced under various conditions, including a, d) pH solutions, b, e) time deposition, and c, f) annealing temperature.

6. Conclusion

In this report, the effect of pH solution, time deposition as well as the annealing temperature onto structural, morphological and optical CZTS layers properties, using chemical bath deposition method deposition was studied. Thermal analysis (DSC/TGA) confirms that the CZTS temperature crystallization is 237.1ºC. X- ray diffraction analysis for thin films of CZTS, proves that the CZTS tetragonal kesterite structure formation with presence of tin oxide and zinc oxide secondary phases, in the films calcined at 300ºC and 350ºC.The kesterite phase is confirmed also by Raman analysis. On the other hand, the layers prepared at 200ºC and 250ºC don't have these secondary phases. Rietveld analysis confirms that the films consist of nanocrystallites. The crystallites sizes are affected by the studied parameters. SEM images show smooth homogeneous surfaces without presence of cracks and voids, especially in the CZTS layers elaborated at 24h and 350ºC.

All films present lower transmittance and higher absorption, the band gap energy is influenced by pH solution and the annealing temperature. It's not affected by the time deposition. It may be concluded that the optimized parameters are 7.8 pH solutions, 48h time deposition and 250ºC of annealing temperature.

References

[1] K. Ito, T. Nakazawa, Japanese Journal of Applied Physics, 27 2094(1988); https://doi.org/10.1143/JJAP.27.2094

[2] C. Shi, G. Shi, Z. Chen, P. Yang, M. Yao, Materials Letters, 73 89-91(2012); https://doi.org/10.1016/j.matlet.2012.01.018

[3] K. Wang, O. Gunawan, T. Todorov, B. Shin, S. Chey, N. Bojarczuk, D. Mitzi, S. Guha, Applied Physics Letters, 97 143508(2010); https://doi.org/10.1063/1.3499284

[4] T. Tanaka, A. Yoshida, D. Saiki, K. Saito, Q. Guo, M. Nishio, T. Yamaguchi, Thin Solid Films, 518 S29-S33(2010); https://doi.org/10.1016/j.tsf.2010.03.026

[5] J.-S. Seol, S.-Y. Lee, J.-C. Lee, H.-D. Nam, K.-H. Kim, Solar energy materials and solar cells, 75 155-162(2003); https://doi.org/10.1016/S0927-0248(02)00127-7

[6] J. Wang, S. Li, J. Cai, B. Shen, Y. Ren, G. Qin, Journal of Alloys and Compounds, 552 418-422(2013); https://doi.org/10.1016/j.jallcom.2012.11.082

[7] T. Tanaka, T. Nagatomo, D. Kawasaki, M. Nishio, Q. Guo, A. Wakahara, A. Yoshida, H. Ogawa, Journal of Physics and Chemistry of Solids, 66 1978-1981(2005); https://doi.org/10.1016/j.jpcs.2005.09.037

[8] B. Shin, O. Gunawan, Y. Zhu, N.A. Bojarczuk, S.J. Chey, S. Guha, Progress in Photovoltaics: Research and applications, 21 72-76(2013); https://doi.org/10.1002/pip.1174

[9] H. Katagiri, K. Jimbo, S. Yamada, T. Kamimura, W.S. Maw, T. Fukano, T. Ito, T. Motohiro, Applied physics express, 1 041201(2008); https://doi.org/10.1143/APEX.1.041201

[10] Y.S. Lee, T. Gershon, O. Gunawan, T.K. Todorov, T. Gokmen, Y. Virgus, S. Guha, Advanced Energy Materials, 5 1401372(2015); https://doi.org/10.1002/aenm.201401372

[11] N. Kamoun, H. Bouzouita, B. Rezig, Thin Solid Films, 515 5949-5952 (2007); https://doi.org/10.1016/j.tsf.2006.12.144

[12] Y. Kumar, G.S. Babu, P.U. Bhaskar, V.S. Raja, Physica status solidi (a), 206 1525-1530 (2009); https://doi.org/10.1002/pssa.200824424

[13] X. Xin, M. He, W. Han, J. Jung, Z. Lin, Angewandte Chemie International Edition, 50 11739-11742(2011); https://doi.org/10.1002/anie.201104786

[14] M.Y. Yeh, C.C. Lee, D.S. Wuu, Journal of sol-gel science and technology, 52 65-68(2009); https://doi.org/10.1007/s10971-009-1997-z

[15] S.S. Mali, P.S. Shinde, C.A. Betty, P.N. Bhosale, Y.W. Oh, P.S. Patil, Journal of Physics and Chemistry of Solids, 73 735-740(2012); https://doi.org/10.1016/j.jpcs.2012.01.008

[16] T.R. Rana, N. Shinde, J. Kim, Materials Letters, 162 40-43(2016); https://doi.org/10.1016/j.matlet.2015.09.100

[17] J. Henry, K. Mohanraj, G. Sivakumar, Optik-International Journal for Light and Electron Optics, (2017); https://doi.org/10.1016/j.ijleo.2017.03.121

[18] K.S. Ramaiah, R. Pilkington, A. Hill, R. Tomlinson, A.-K. Bhatnagar, Materials chemistry and physics, 68 22-30(2001); https://doi.org/10.1016/S0254-0584(00)00281-9

[19] J. Hiie, T. Dedova, V. Valdna, K. Muska, Thin Solid Films, 511 443-447 (2006); https://doi.org/10.1016/j.tsf.2005.11.070

[20] E. Çetinörgü, C. Gümüş, R. Esen, Thin Solid Films, 515 1688-1693(2006); https://doi.org/10.1016/j.tsf.2006.06.004

[21] C. Gao, T. Schnabel, T. Abzieher, C. Krämmer, M. Powalla, H. Kalt, M. Hetterich, Thin Solid Films, 562 621-624(2014); https://doi.org/10.1016/j.tsf.2014.04.030

[22] E. Subramaniam, G. Rajesh, N. Muthukumarasamy, M. Thambidurai, V. Asokan, D. Velauthapillai, Indian Journal of Pure & Applied Physics.;52(9):620-624 (2014)

[23] R. D'Angelo Bandres, Preparation and characterization of Cu2-xZn1+ ySnS4 for thin films solar cells, in, University of Trento, (2016)

[24] K. Rawat, P. Shishodia, Advanced Powder Technology, 28 611-617(2017); https://doi.org/10.1016/j.apt.2016.11.013

[25] K. Moriya, K. Tanaka, H. Uchiki, Japanese Journal of Applied Physics, 46 5780(2007); https://doi.org/10.1143/JJAP.46.5780

[26] V. Kumar, S. Kumari, P. Kumar, M. Kar, L. Kumar, Adv. Mater. Lett, 6 139-147 (2015); https://doi.org/10.5185/amlett.2015.5632

[27] L. Chen, T. Mashimo, E. Omurzak, H. Okudera, C. Iwamoto, A. Yoshiasa, The Journal of Physical Chemistry C, 115 9370-9375(2011); https://doi.org/10.1021/jp111367k

[28] D. Haouanoh, R. Zaïr, M. Toubane, F. Bensouici, A.P. Samantilleke, R.Z. TalaIghil, Study of Temperature and Concentration Effects for CZTS Layers using Spray Pyrolysis, in: 2017 International Renewable and Sustainable Energy Conference (IRSEC), IEEE, , pp. 1-6(2017); https://doi.org/10.1109/IRSEC.2017.8477430

[29] M. Guc, S. Levcenko, I.V. Bodnar, V. Izquierdo-Roca, X. Fontane, L.V. Volkova, E. Arushanov, A. Pérez-Rodríguez, Scientific reports, 6 1-7 (2016); https://doi.org/10.1038/srep19414

[30] M. Dimitrievska, A. Fairbrother, X. Fontané, T. Jawhari, V. Izquierdo-Roca, E. Saucedo, A. Pérez-Rodríguez, Applied Physics Letters, 104 021901(2014); https://doi.org/10.1063/1.4861593

[31] S. Bouhouche, F. Bensouici, M. Toubane, A. Azizi, A. Otmani, K. Chebout, F. Kezzoula, R. Tala-Ighil, M. Bououdina, Materials Research Express, 5 056407(2018); https://doi.org/10.1088/2053-1591/aac4e8

[32] F. Aslan, A. Göktaş, A. Tumbul, Materials Science in Semiconductor Processing, 43 139-143(2016); https://doi.org/10.1016/j.mssp.2015.12.011

[33] M. Toubane, R. Tala-Ighil, F. Bensouici, M. Bououdina, M. Souier, S. Liu, W. Cai, A. Iratni, Materials Research Express, 4 035023(2017); https://doi.org/10.1088/2053-1591/aa61cf

[34] J. Manifacier, M. De Murcia, J. Fillard, E. Vicario, Thin Solid Films, 41 127-135(1977); https://doi.org/10.1016/0040-6090(77)90395-9

[35] S.T. Tan, B. Chen, X. Sun, W. Fan, H. Kwok, X. Zhang, S. Chua, Journal of Applied Physics, 98 013505 (2005); https://doi.org/10.1063/1.1940137

[36] M.-M. Bagheri-Mohagheghi, N. Shahtahmasebi, M. Alinejad, A. Youssefi, M. Shokooh-Saremi, Physica B: Condensed Matter, 403 2431-2437(2008); https://doi.org/10.1016/j.physb.2008.01.004